

## Albedo-corrected Parameterized Equivalence Constants for Cross-section Correction in Nodal Calculation

Woosong Kim and Yonghee Kim\*

Dept. of Nuclear and Quantum Eng., KAIST, 291 Daehak-ro, Yuseong-gu, Daejeon, Korea, 34141

\*Corresponding author: yongheekim@kaist.ac.kr

**Abstract** – This paper introduces the albedo-corrected parameterized equivalence constants (APEC) method, a new method for correcting the homogenized two-group cross-sections of the PWR fuel assemblies by taking into account neutron leakage. In order to eliminate the two-group cross-section error in the conventional homogenization method, the APEC method is proposed which parameterizes the homogenized two-group cross-sections in terms of an integrated albedo information current-to-flux ratio (CFR). In order to obtain physically meaningful CFR boundary conditions for the APEC method, small color-set models are introduced and their characteristic features are discussed. In the case of baffle-facing fuel assemblies, slightly modified APEC formulas are introduced to deal with the strong spectral interaction between fuel assembly and the baffle-reflector region in PWRs. In addition, an improved APEC function is developed by explicitly accounting for the neutron spectrum change in a fuel assembly in terms of a spectral index defined as the fast-to-thermal flux ratio. A two-node NEM code developed at the Korea Advanced Institute of Science and Technology (KAIST) was used for the nodal code to implement the APEC method in conjunction the partial-current based CMFD (p-CMFD) acceleration. For the test of the proposed APEC functions, nodal analyses are performed for a small modular reactor (SMR) core. For the analyses, a 2D transport code, DeCART2D, was used in this work. The SMR benchmark analyses showed that the APEC method significantly improves nodal accuracy with a marginal increase of computing cost.

### I. INTRODUCTION

Nodal equivalence theory is a cornerstone of modern nuclear reactor analysis in which the heterogeneous core is simplified into a number of homogenized fuel assemblies (FAs). The foundational idea supporting the theory is the imperative to preserve equivalence between the original heterogeneous assembly and a simplified homogenized assembly in terms of their reaction rates and node interface currents. Today, simplified equivalence theory (SET) [1] is one of the most widely used of these techniques due to its computational efficiency. For the application of SET to a two-step procedure, single assembly transport analysis is performed using reflective boundary conditions. Based on this infinite lattice calculation, a single set of few-group homogenized parameters can be evaluated including cross-sections (XSs) and discontinuity factors (DFs). As an infinite lattice has no neutron leakage and is unphysical, an appropriate leakage correction considering the critical spectrum in actual reactor cores has to be applied to the evaluation of the parameters [2].

Although SET is very efficient, the core nodal calculation accuracy based on a single assembly homogenization is quite limited when the node interface current is not close to zero and the neighborhood effect is rather strong in practical cores [3]. Recently, W. Heo quantified the assembly environment effect on the homogenized two-group constants in a typical PWR (pressurized water reactor) core by way of Monte Carlo core analysis [4]. As a result, it is clarified that the homogenized

two-group constants are clearly position-dependent and a correction is required to improve the accuracy of the multi-dimensional reactor analysis.

To overcome the limitation of current methods to generate few-group homogenized group constants, several approaches to functionalize the equivalence constants have been suggested. These approaches seek to improve the accuracy of whole-core solutions while maintaining the advantage of the conventional two-step procedure. These include boundary perturbation theory [5,6], functionalized interface discontinuity factors according to pin cell environment [7] that are not applicable to assembly homogenization, the rehomogenization method [8] that provides the successful correction of XSs based on the nodal expansion of neutron flux, and the leakage feedback method [9] in which XSs are corrected by using a definition of leakage fraction.

In our previous study of equivalence constant functionalization [10], the functionalized discontinuity factor was considered first. Here, the DF is functionalized with respect to the current-to-flux ratio (CFR) of the FA surface, but the correction of the DF alone has only a marginal effect on improving the nodal accuracy. In a recent study by W. Kim and Y. Kim [11,12], the Albedo-corrected Parameterized Equivalence Constants (APEC) method was proposed by focusing on the two-group XS correction. The homogenized two-group XSs are parameterized as a function of node-average current-to-flux ratio (CFR) to uniquely represent the albedo information of the node interface. Ref. 11 shows the feasibility that the assembly XS

correction by the APEC method can clearly improve accuracy of the homogeneous solutions of a 2-D PWR benchmark problem.

Since the XS correction is much more effective in enhancing the nodal accuracy than the DF correction, this paper only develops the APEC method of XS correction for the nodal diffusion calculations with the main objective of this work being to validate the effectiveness of XS correction by the APEC method. The 2-D Method of Characteristics (MOC) lattice code, DeCART2D [13], was used for the lattice calculations to determine the two-group XSs with different lattice boundary conditions and the APEC method is implemented in a two-node Nodal Expansion Method (NEM) code [14] developed in our research group. Various albedo information at the FA boundary can be given by way of a color-set model where the FA in question is surrounded by different FAs. As a result, the two-group XS change due to boundary albedo information can be functionalized by fitting APEC functions to the color-set calculations results. The function fitting is done by solving system of equations or using least square method. The nodal calculation accuracy is examined by comparing the multiplication factor, assembly normalized power distribution, and assembly two-group XSs.

## II. ALBEDO-CORRECTED PARAMETERIZED EQUIVALENCE CONSTANTS (APEC) METHOD

The conventional flux-weighted constants (FWCs) can be quite different from the reference values which are obtained from the whole-core heterogeneous calculation. However, if one can generate the few-group constants as a function of neutron leakage through FA interfaces, it is expected that the XSs can be corrected by using the actual leakage information during the iterative core calculations. The resulting nodal equivalence for the homogenized FAs will then be improved, leading to a more accurate core analysis. With this kind of considerations of the actual interface conditions between FAs, the ad hoc critical spectrum correction may be eliminated in the conventional lattice calculations and the current two-step procedures can be applied to not only critical condition but also to any non-critical situations.

### 1. Albedo-only Functionalization of Fuel Assembly XS

The leakage effects on the homogenized two-group XSs are considered by using the albedo information of the assembly surfaces. A previous study [12] showed that if a FA is symmetric, the two-group homogenized XS have a strong relationship with the assembly-wise CFR at assembly  $m$ , defined as below:

$$CFR_g^m = \sum_s J_{g,m}^s / \sum_s \phi_{g,m}^s, \quad (1)$$

where the numerator is the summation of the  $g^{th}$  group surface outward net currents of assembly  $m$  and the denominator is the summation of the  $g^{th}$  group surface fluxes of assembly  $m$ . In this paper, the assembly-wise CFR is preferred to the albedo because it is a more explicit definition of neutron leakage. It should be noted that the CFR is a normalized parameter representing a surface-integrated leakage of the FA.

In fact, the albedo is another expression of CFR and can be explicitly derived with the diffusion approximation [15]. Eqs. (2) and (3) show the relationship between the CFR and albedo. Figure 1 shows the CFR plotted over the albedo. In Fig. 1, one notes that the CFR ranges from about -0.2 to 0.5. In actual cores, the range of the CFR values will be much narrower than the whole range. The CFR is zero when there is no net neutron leakage and XS correction is not necessary. If the CFR has a positive value for a FA, there should be a net outgoing leakage of neutrons from the FA. Meanwhile a negative CFR indicates that the neutron in the group has a net incoming flow from neighboring FAs. Both positive and negative CFR will change the neutron spectrum and the homogenized two-group constants should be different from the single assembly results.

$$\alpha = \frac{J^-}{J^+} = \frac{\frac{1}{4}\phi - \frac{1}{2}J}{\frac{1}{4}\phi + \frac{1}{2}J}, \quad (2)$$

$$\frac{J}{\phi} = \frac{1(1-\alpha)}{2(1+\alpha)}. \quad (3)$$

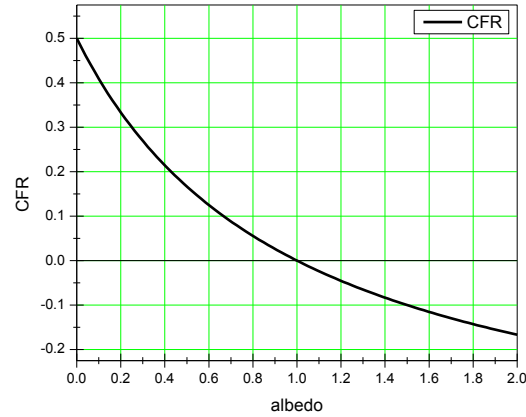


Fig. 1. CFR vs. albedo in diffusion approximation.

In the standard and simplest APEC method, the XS changes due to the non-zero node interface leakage are functionalized with the CFR as follows for node  $m$ , reaction  $x$ , and group  $g$ :

$$\Delta\Sigma_{x,F}^m = a1_{x,F} CFR_F^m + a2_{x,F} CFR_T^m \quad (4a)$$

$$\Delta\Sigma_{x,T}^m = a1_{x,T} CFR_T^m + a2_{x,T} (CFR_T^m)^2 \quad (4b)$$

$$\Sigma_{x,g}^m = \Sigma_{x,g}^0 + \Delta\Sigma_{x,g}^m \quad (5)$$

where  $\Sigma_{x,g}^m$  is the corrected XS,  $\Sigma_{x,g}^0$  is the FWC XS by single assembly calculations, and  $\Delta\Sigma_{x,g}^m$  is the XS change in Eq. (4). The fast group XS change is a linear function of both fast and thermal group CFRs. This is because the energy spectrum change for the wide fast group is dependent on both fast and thermal groups. In particular, it is obvious that down-scattering XS change should depend on both fast group and thermal group leakages. On the other hand, the thermal group XS change is a quadratic polynomial function of the thermal group CFR only. Our experience has shown that the thermal group XS has a non-linear dependence on the thermal CFR value and is insensitive to the fast-group CFR.

In order to obtain the two parameters,  $a1_{x,g}$  and  $a2_{x,g}$ , the change in XS data as a function of different CFR values is required. However, arbitrary albedo boundary conditions on a single FA cannot provide good results because they are likely to be non-physical boundary conditions. In order for the CFR at the boundary to be physically meaningful, it is necessary to change the CFR by arranging the actual environment around the FA so that physical CFRs are obtained. This enables a more accurate APEC functionalization and can be applied to a wider range of problems. To find physically acceptable CFR conditions, we suggest using the checkerboard type color-set problem shown in Fig. 2 in addition to the single assembly problem. A color-set is a small problem comprised of several FAs. For a certain FA, a non-zero CFR can be given by surrounding it with different FAs. Different surrounding FAs will give different CFRs at the boundary of the FA of interest. Then, the parameters in the APEC function can be determined by fitting a function to the change in XS and different CFR values.

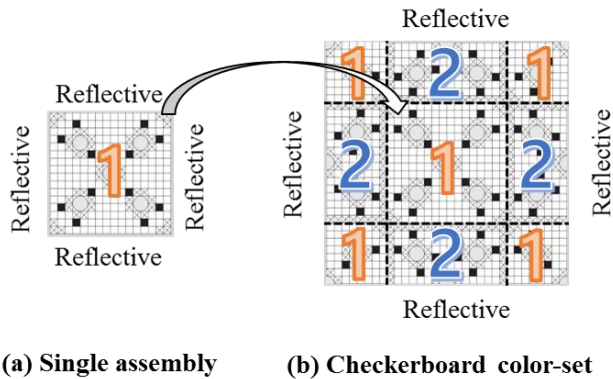


Fig. 2. Single assembly (a) and checkerboard color-set problems (b) for FAs in the inner core region.

As the APEC XS correction functions have two unknowns for both fast and thermal groups, only two color-set calculations are necessary for each FA. Of course, more reliable coefficients can be available if more color-set calculations are considered. However, the minimum number of color-set calculations are considered in this study to see the performance of the APEC XS update with minimal computational burden. It is noteworthy that the total number of required color-set calculations can be reduced by using one color-set results for both FAs in the color-set problem.

#### A. Color-set Model Selection

The color-set models for APEC parameter fitting must be carefully selected to ensure the best performance with minimal additional computational cost. First of all, because extrapolation is not as good as interpolation in view of functional approximation, the range of the CFR values for the color-set calculations should be wide enough to cover all possible CFRs in the core. If two color-set calculations provide appropriate minimum and maximum CFRs, the resulting APEC function will be good and additional color-set calculations are not necessary. Hence, both the magnitude and direction of the CFRs are important for the function fitting. Another important aspect of color-set model selection is that all FAs in a color-set model should be similar to the ‘actual’ FA design inside the core. This constraint is required to correctly reflect the neutronic characteristics of the actual core in the XS functionalization. Several guidelines recommended for proper color-set model selection are listed below:

1. Each color-set should have at least two different types of FAs. They should differ in terms of fuel burnup, fuel enrichment, amount of burnable poison, and insertion of the control rods. This maximizes the range covered by the CFR calculated by the color-set calculation.
2. The second color-set model of a FA should be selected to have a CFR in the opposite direction or sign to the first color-set model.
3. When determining the CFR direction of the color-set model, improbable directions should be ignored. For example, we do not consider the net-incoming of fast neutron (negative CFR) of a FA with a very high fuel enrichment or the net-outgoing of thermal neutrons (positive CFR) of a rodged FA.
4. A minimum number of color-set calculations is recommended to minimize the additional computing time. When the number of color-set calculations and the number of APEC parameters are equal, the system of equations can be solved to obtain the unique solution. However, if a FA is used for other FA’s color-set analyses, least square method fitting can be used for the overdetermined

problem.

A good example of a color-set model is the FA surrounded by control rod inserted FAs. This model will provide a boundary condition which is physically meaningful while giving a large positive CFR to the FA at the center. Physically meaningful means that it is a boundary condition with a realistic spectrum that is likely to be in an actual core. If one needs a wider range of CFR for a certain FA, a different boundary condition other than all-reflective, (such as vacuum boundary condition) can be applied to the color-set model. This instance is not considered in the current study.

### B. Baffle-reflector-facing Fuel Assembly

When a FA is facing a baffle-reflector region, it has a very different neutron energy spectrum and spatial power distribution from one in the inner core region or an infinite lattice. Therefore, different fitting functions and color-set problems are needed to functionalize XS changes for such special FAs. To consider the strong effect of the baffle-reflector in PWRs, a constant term is added to the basic APEC fitting function as given in Eq. (6).

$$\Delta\Sigma_{x,F}^m = a1_{x,F} CFR_F^m + a2_{x,F} CFR_T^m + c_{x,F} \quad (6a)$$

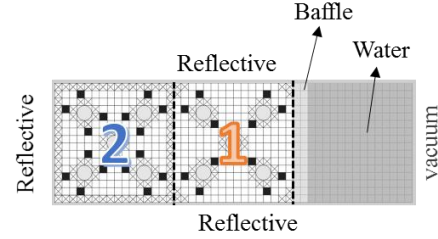
$$\Delta\Sigma_{x,T}^m = a1_{x,T} CFR_T^m + a2_{x,T} (CFR_T^m)^2 + c_{x,T} \quad (6b)$$

where  $c_{x,g}$  is the constant term. As there are 3 parameters, 3 color-set calculations are necessary for fitting the XS change in the baffle-facing FA.

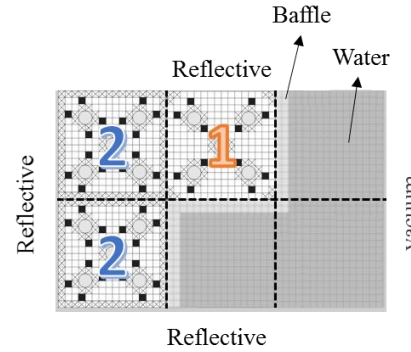
Figure 3 presents the new color-set problems including the traditional baffle-reflector spectral geometry. When a FA is neighboring a flat baffle-reflector region, three color-set calculations are performed with the flat baffle-reflector model in Fig. 3-(a). In this traditional color-set analysis, different FAs are placed in the FA2 position in Fig. 3-(a) to simulate different albedo conditions on the interface with the main FA in position 1. If a FA is facing an L-shape baffle, three color-set analyses using the L-shape baffle-reflector model in Fig. 3-(b) are performed. In this case, changing the two FAs in position 2 simulates different CFR conditions. The XS differences between the infinite lattice calculation and color-set calculations are fitted to Eq. (6) for evaluating corresponding parameters. As a result, different parameters will be applied to the same type of FA depending on the shape of the baffle to determine more accurate XS corrections.

One more advantage of using the L-shape baffle-reflector color-set model is that very accurate baffle-reflector two-group parameters can be obtained for the L-shape baffle-reflector region from the same color-set analysis. Fig. 3 shows four types of baffle-reflector regions in the color-set models, one in the flat baffle-reflector model and three in the L-shape baffle-reflector model. The flat

baffle-reflector region in the L-shape color-set shown in Fig. 3-(b) has the same shape as the baffle-reflector in the flat baffle-reflector color-set shown in Fig. 3-(a), but they have different two-group XSs because the environment is different. If a barrel surrounds the core, it can be included in the color-set model and used to evaluate the two-group parameters more accurately.



(a) Flat baffle-reflector model



(b) L-shape baffle-reflector model

Fig. 3 Color-set problem for FAs facing flat baffle-reflector (a) and L-shape baffle-reflector (b)

## 2. Energy Spectrum Consideration

Although the standard and simple APEC formulas in Eq. (4) significantly correct the two-group XSs, the neutron spectrum change can be explicitly taken into account to improve the performance of the APEC method. The degree of energy spectrum change in a FA due to neighbors can be represented by the change in the two-group Spectral Index (SI) in Eq. (7). In this improved APEC, variation of the SI is considered in the APEC function for FAs in the inner core region in the following way:

$$SI = \bar{\phi}_{fast} / \bar{\phi}_{thermal} \quad (7)$$

$$\Delta SI^m = SI^m - SI^0 \quad (8)$$

$$\Delta\Sigma_{x,F}^m = a1_{x,F} CFR_F^m + a2_{x,F} CFR_T^m + a3_{x,F} \Delta SI^m \quad (9a)$$

$$\Delta\Sigma_{x,T}^m = a1_{x,T} CFR_T^m + a2_{x,T} (CFR_T^m)^2 + a3_{x,T} \Delta SI^m \quad (9b)$$

where  $\bar{\phi}_g$  is node-average flux,  $\Delta SI^m$  is the difference

between the SI at position  $m$  ( $SI^m$ ) and the SI of the infinite lattice calculation ( $SI^0$ ). As an extra coefficient is added to the original APEC function, additional color-set calculations are necessary for the function fitting of the added parameters. In this work, 4 color-set calculation results are used for determining the 3 parameters in Eq. (9) by using the least-square method. The reason for 4 color-set calculations instead of 3 color-set calculations is to obtain a sufficiently wide range of values for both CFR and SI.

Further improvement of the XS correction using the SI value will be more effective for the fast group because the energy spectrum is more important for the fast group condensation due to its much wider range and epithermal resonance peaks. However, it should be noted that the APEC function for baffle-facing FA does not need to consider the SI. The APEC function of a baffle-facing FA is already very effective without explicit consideration of the SI because of its constant term  $c_{x,g}$  and the detailed baffle-reflector model which reflects the actual spectral situation quite well. The FA XS correction by using Eq. (6) and (9) described in this section is named the APEC-SI method.

### 3. Implementation to Two-node NEM Nodal Calculation

The APEC method is implemented in a two-node Nodal Expansion Method (NEM) code developed in our research group. The impact of the APEC XS update on the nodal analysis accuracy is demonstrated by comparing core calculation results with conventional FWC XSs. While the coarse-mesh finite difference (CMFD) method [16] is a very effective and popular acceleration scheme for nodal calculations, the partial current-based CMFD (p-CMFD) method [17,18] was chosen for our APEC method implementation of the nodal calculation acceleration. In the p-CMFD acceleration method, there are two correction factors for each node interface to preserve both incoming and outgoing partial currents while the CMFD method preserves only net current. Since partial currents are preserved in the p-CMFD method, all surface net current, surface flux, and albedo are preserved between the high-order NEM kernel and the coarse mesh FDM. Therefore, the APEC XS correction by node interface albedo from NEM kernel can be adapted during the FDM outer iteration. The conventional CMFD method is not suitable for use with the APEC method because it does not preserve surface flux and albedo. Also, the p-CMFD method always provide more stable acceleration than the CMFD method [19].

The flowchart of the APEC method implemented two-node NEM p-CMFD nodal calculation is shown in Fig. 4. During the nodal calculation, the FA XSs are updated by the APEC method when the p-CMFD correction factors are updated. Therefore, the APEC XS update does not need any additional iteration loops and the convergence speed is comparable to the conventional nodal calculation without the APEC method implementation. Also, because the APEC XS update is only solving linear equations, its computing

cost is almost negligible.

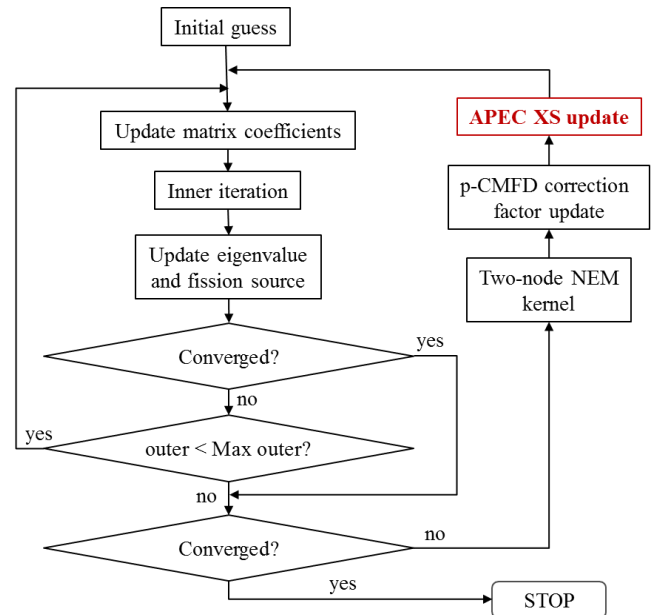
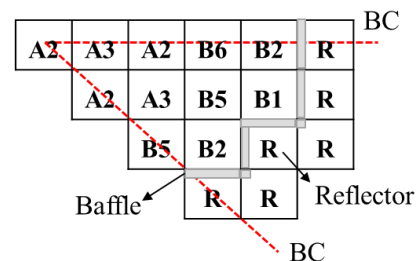


Fig. 4. Flowchart of the two-node NEM code with APEC method

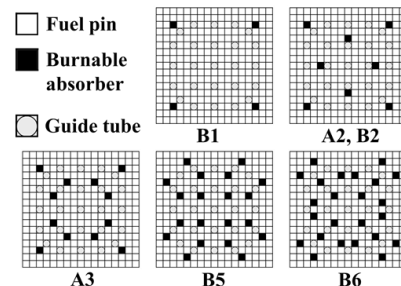
## III. NUMERICAL RESULTS

### 1. SMR Initial Core Problem

To test the effectiveness of the APEC method, a small modular reactor (SMR) initial core was selected as a benchmark problem, which is shown in Fig. 5.



(a) Core configuration



(b) Fuel assembly configuration

Fig. 5. SMR initial core problem

The validity of conventional two-step processes for a small size reactor is relatively low due to the large neutron leakage at the core boundary. In the SMR problem, many Gd<sub>2</sub>O<sub>3</sub> burnable absorber rods are loaded making the problem more difficult to analyze using standard two-step methods. There are 6 types of 17x17 FAs in the SMR core, as shown in Fig. 5. For A2- and A3-type FAs, U enrichment is 2.8 w/o and is about 4.9 w/o for other FAs. The reference heterogeneous global core (1/8<sup>th</sup> symmetry) calculation took about 1 hour and 6 minutes on a Windows-based i7-6700K CPU. In the reference DeCART2D analysis, the coolant and fuel temperatures were both 600 K, and the MOC ray spacing was 0.02 cm with 8 azimuthal angles for 90° and 2 polar angles for the hemisphere.

## 2. Lattice Calculations for APEC Method

Lattice calculations are performed for 6 single assembly models and 19 color-set models for the APEC functionalization. As shown in Table I, the color-set models for the basic APEC function consist of 5 checkerboard models, 3 flat baffle models and 6 L-shape baffle models. There are 15 combinations of color-set models that can be made of 6 FAs, but instead of calculating all of these combinations, only 5 color-set models were calculated for the basic APEC function. Additional color-set models for the APEC-SI function consist of 5 checkerboard models shown in Table II. The DeCART2D calculation time for each lattice calculation was about 16 seconds for a single FA, about 1 minute for checkerboard color-set models, about 8 minutes for flat baffle-reflector color-set models, and about 18 minutes for L-shape baffle-reflector color-set models.

Table I. SMR core color-set models for basic APEC method

Type of color-set model	Set of FAs in color-set (FA1, FA2)
Checkerboard	(A2,A3), (A2,B5), (A3,B6), (B1,B5), (B1,B6)
Flat baffle	(B2,A2), (B2,B2), (B2,B6)
L-shape baffle	(B1,A2), (B1,B1), (B1,B5), (B2,A2), (B2,B2), (B2,B6)

Table II. Additional color-set models for APEC-SI method (FA1, FA2)

Type of color-set model	Set of FAs in color-set (FA1, FA2)
Checkerboard	(A2,A3), (A2,B5), (A3,B6), (B1,B5), (B1,B6)

In Tables III and IV, the assembly-wise CFRs obtained from the 19 color-set calculations are summarized together with the FAs and the paired assemblies. Different assembly-

wise CFR values were obtained depending on neighboring FAs. One can observe in Tables III and IV that CFR values from color-set calculations are quite small, even when two very different FAs are paired to provide a wide range of CFRs. The range of assembly-wise CFR from checkerboard color-sets is -0.018~0.01 for fast group and -0.035~0.035 for thermal group. It can be expected that the range of assembly-wise CFR values in the actual core will be very narrow in the inner core region. It is also noticeable that the baffle-facing FA always has a positive CFR due to the strong neutron leakage to the baffle region, as shown in Table IV. Also, the FA facing L-shape baffle-reflector has a clearly larger CFR than the FA facing flat baffle-reflector. However, the maximum value of CFR is still only about 0.041.

Table III. Assembly-wise CFR from checkerboard color-set calculations

FA1	FA2	CFR <sub>1</sub>	CFR <sub>2</sub>	ΔSI
A2	A3	2.86E-03	1.46E-03	3.94E-02
	B1	-1.53E-02	2.76E-02	2.48E-01
	B5	-7.05E-03	3.43E-02	3.78E-01
	B6	-5.07E-03	3.54E-02	4.00E-01
A3	A2	-2.86E-03	-1.46E-03	-4.25E-02
	B1	-1.82E-02	2.60E-02	2.26E-01
	B5	-1.00E-02	3.28E-02	3.65E-01
	B6	-8.05E-03	3.38E-02	3.90E-01
B5	A2	7.05E-03	-3.43E-02	-5.49E-01
	A3	1.00E-02	-3.28E-02	-4.87E-01
	B1	-8.56E-03	-7.19E-03	-1.97E-01
	B6	2.08E-03	1.03E-03	4.00E-02
B6	A2	5.07E-03	-3.54E-02	-6.17E-01
	A3	8.05E-03	-3.38E-02	-5.52E-01
	B1	-1.06E-02	-8.24E-03	-2.48E-01
	B5	-2.08E-03	-1.03E-03	-3.83E-02

Table IV. Assembly-wise CFR from baffle-reflector including color-set calculations

FA1	FA2	CFR <sub>1</sub>	CFR <sub>2</sub>	ΔSI
B1 (L-shape Baffle)	A2	2.98E-02	1.89E-02	3.27E-01
	B1	8.56E-03	3.06E-02	2.62E-01
	B5	2.63E-02	3.95E-02	5.16E-01
B2 (flat baffle)	A2	1.67E-02	2.55E-03	1.02E-01
	B2	4.73E-03	1.32E-02	1.33E-01
	B6	1.70E-02	2.01E-02	3.33E-01
B2 (L-shape baffle)	A2	2.49E-02	1.61E-02	2.67E-01
	B2	8.44E-03	3.03E-02	2.77E-01
	B6	2.53E-02	3.92E-02	5.37E-01

The fast group APEC functions are compared for fast group fission XS ( $\Delta v\Sigma_f$ ) of the B5-type FA in Fig. 6 and their coefficients are given in Table V. The fast group  $\Delta v\Sigma_f$  is defined as the XS of color-set calculations minus the FWC of the single assembly. In Fig. 6, fast group  $\Delta v\Sigma_f$  from color-set calculations are indicated by black dots while the fitted

APEC functions are plotted with solid black lines. While the basic APEC function (solid line) is fitted using only two color-set data, APEC-SI function (dotted line) used four color-set data. In Fig. 6, the APEC-SI function is expressed only for the fast and thermal group CFRs, ignoring the SI term. Therefore, it shows very different values from the basic APEC functions, but it has good agreement with the  $\Delta v\Sigma_f$  from color-set and core calculations if the SI term is included.

Figure 7 shows the thermal group  $\Delta v\Sigma_f$  for the B5 FA predicted by the two APEC functions in comparison with the results of the color-set and reference core calculations. In this case, The APEC-SI looks slightly different from the basic APEC, but it also agrees very well with the reference values once the SI term is included.

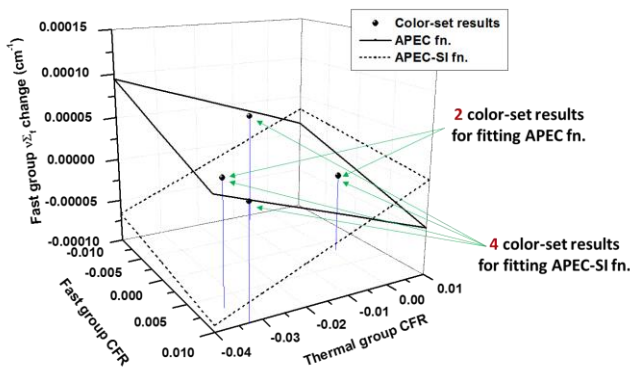


Fig. 6. Fast group  $\Delta v\Sigma_f$  APEC function fitting (B5 FA)

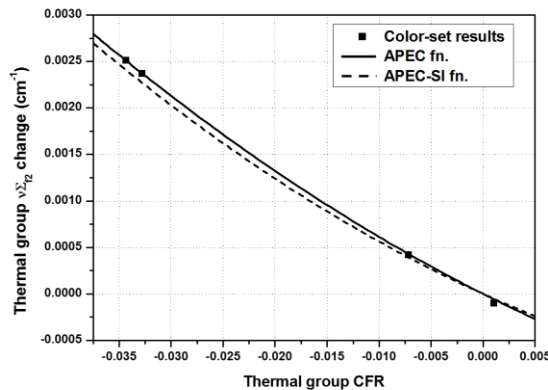


Fig. 7. Thermal group  $\Delta v\Sigma_f$  APEC function fitting (B5 FA)

Table V. Coefficients of APEC functions at B5 FA

	coefficients	$v\Sigma_{f1}$	$v\Sigma_{f2}$
APEC	a1 (CFR <sub>1</sub> )	-3.006E-03	-5.488E-02
	a2 (CFR <sub>2</sub> )	-1.600E-03	5.289E-01
APEC-SI	a1 (CFR <sub>1</sub> )	-1.343E-03	-5.071E-02
	a2 (CFR <sub>2</sub> )	1.991E-03	5.651E-01
	a3 ( $\Delta$ SI)	-2.037E-04	-1.922E-04

### 3. Nodal Calculations

For the comparison, the two-group XSs for the following FA types are used for in a core simulation: 1) the conventional FWC from single FA calculation, 2) basic APEC correction, 3) improved APEC with Spectral Index (SI) consideration, and 4) reference XS from core transport calculations. For all 4 cases, conventional ADFs (assembly discontinuity factor) are used along with 4 position dependent baffle-reflector XS from the color-set calculations. In the nodal calculation, 2x2 nodes per assembly were used and the convergence criteria for  $k_{eff}$  and fission source were both set to  $10^{-10}$ . The nodal calculations are performed by the parallel computing system consisting of 8 nodes (Intel® Xeon® CPU E5-2697 v3 @ 2.6GHz), while only single core calculations are used in this study.

The APEC XS correction showed improvement in the accuracy of  $k_{eff}$  and assembly power distribution as shown in Table VI. Reactivity error decreased by over 90%, maximum assembly power error decreased by over 40%, and assembly power RMS error decreased by 39%. The number of outer iterations and calculation time are very similar with the APEC method implemented calculation, still finishing faster than even the conventional method calculation. The APEC XS correction showed results similar to those using reference value XS because the APEC XS correction was very close to the reference value. By applying an improved APEC method, further improvement in accuracy can be achieved over the already excellent performance shown by the basic APEC method. Of these, APEC-SI showed best performance when considering the energy spectrum.

Table VI. Nodal calculation results of SMR core

	$k_{eff}$	$\Delta\rho$ (pcm)	assembly power RMS error (%)	assembly power Max. error(%)
DeCART2D	1.144206			
FWC	1.145685	112.8	1.41	2.42
APEC	1.144335	9.8	0.86	1.43
APEC-SI	1.144270	4.9	0.74	1.29
Ref. XS	1.144065	-10.7	0.64	1.17

The assembly normalized power distributions are also compared. While the reference assembly power distribution from the DeCART2D calculation is shown in Fig. 8, the assembly power error distribution is shown in Fig. 9. The APEC method showed a similar power distribution to that using the reference XS because of accurate XS correction by the APEC method. Again, the results of APEC-SI showed the smallest error. The assembly XS relative error is evaluated for every FA and its RMS values are compared in Table VII. The APEC method reduced the XS error by more

than 70%, especially the error of the important thermal group XS which decreased by more than 90%. Improved APEC methods showed better correction in the fast group fission XS and down-scattering XS than in the basic APEC method.



Fig. 8. Reference assembly normalized power distribution

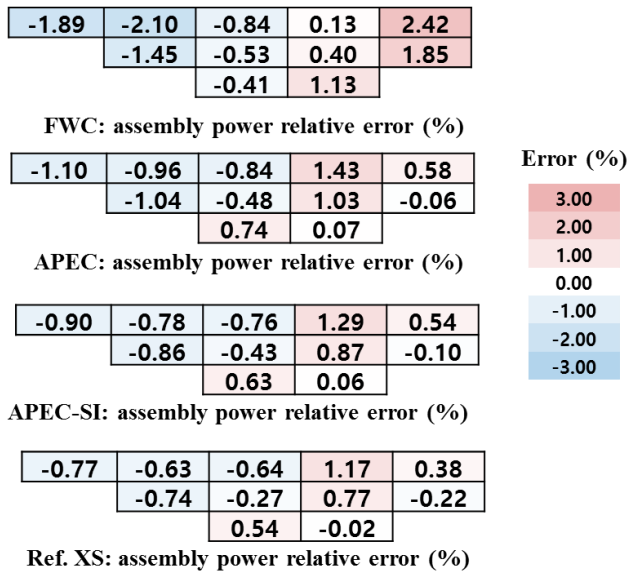


Fig. 9. Relative error of assembly normalized power distribution

Table VII. RMS error of assembly-wise CFR and XS in the SMR core

	FWC (%)	APEC (%)	APEC-SI (%)	Ref. XS (%)
CFR <sub>1</sub>	4.71	5.59	4.96	4.10
CFR <sub>2</sub>	18.20	11.98	12.24	12.30
D <sub>1</sub>	0.36	0.10	0.12	0.00
D <sub>2</sub>	0.23	0.01	0.02	0.00
Σ <sub>a1</sub>	0.36	0.03	0.04	0.00
Σ <sub>a2</sub>	0.41	0.02	0.03	0.00
vΣ <sub>f1</sub>	0.47	0.12	0.07	0.00
vΣ <sub>f2</sub>	0.56	0.05	0.04	0.00
Σ <sub>s1→2</sub>	0.92	0.09	0.05	0.00
Σ <sub>s2→1</sub>	1.89	0.10	0.15	0.00

The convergence behavior is analyzed in terms of  $k_{eff}$  and two-group XS. After the APEC XS correction, the  $k_{eff}$  value converged close to the reference solution without any convergence issue as shown in Fig. 10. The convergence behavior of the B6 FA XS using the basic APEC and APEC-SI update is also shown in Fig. 11. In both methods, the two-group XS converged close to the reference value starting from the initial FWC value, while the XS converged to more accurate values when using the APEC-SI method.

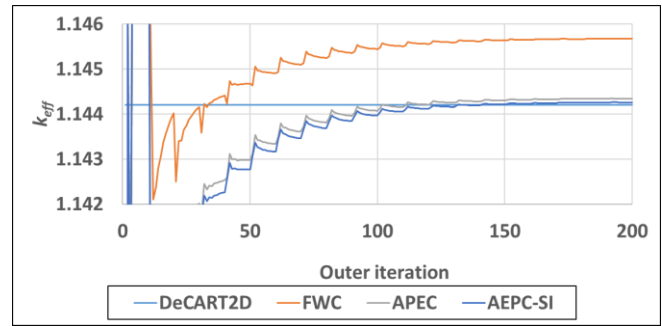
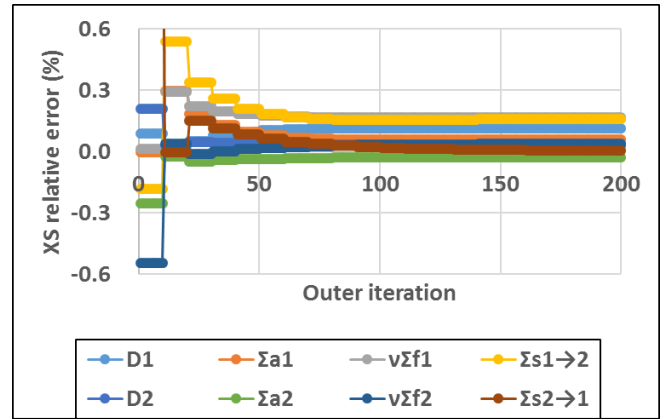
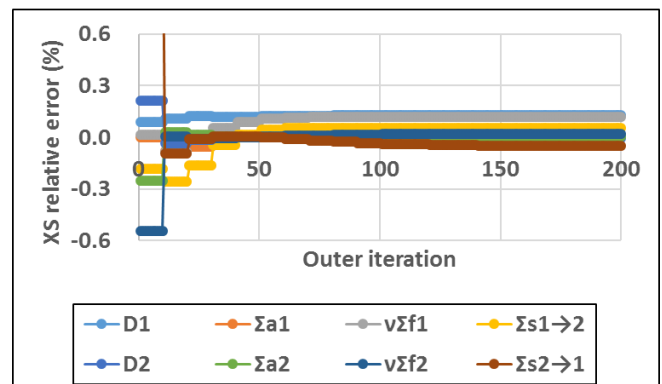


Fig. 10.  $k_{eff}$  convergence behavior in the SMR core



(a) APEC



(b) APEC-SI

Fig. 11. XS convergence behavior (B6 FA in the SMR core)

A. Variant core test

If the APEC method corrects XS close to the reference XS, it should work for any core configuration and can be broadly applied for general purpose applications. To demonstrate this, the APEC method is applied to the SMR's variant cores shown in Fig. 12. A random number generator was used to determine which FA is loaded at each position of variant cores. The lattice calculations including color-set models and the corresponding APEC function parameters used in this test are the same as the previous SMR initial core problem. The FAs facing baffle-reflector were limited to those which have corresponding APEC parameters.

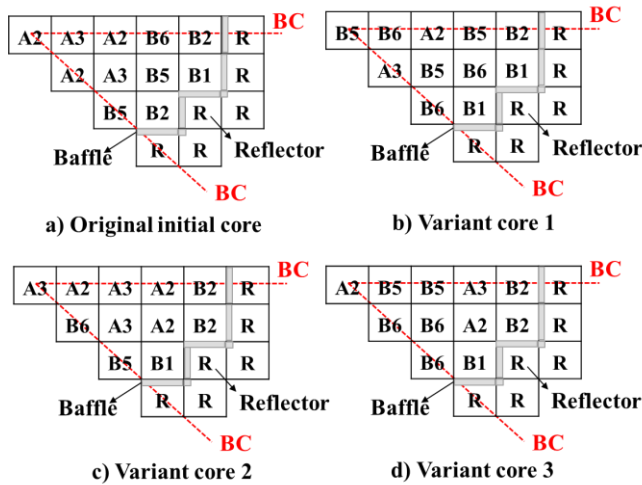


Fig. 12. Configuration of SMR's original and variant cores

Without any additional lattice calculations, nodal calculations are performed for three variant cores. Tables VIII, IX, and X show that the nodal accuracy is significantly improved by APEC XS correction for all three variant cores without convergence issues and no additional calculation time. Also, the APEC-SI method showed noticeably reduced reactivity error than the simple standard APEC methods. Therefore, it can be regarded that a well-determined APEC function with an appropriate color-set model can improve the nodal calculation accuracy for any arbitrary core configuration and further accuracy improvement is achievable by using the APEC-SI method considering more color-set models.

The RMS error of the FA two-group XS and CFR is also compared in Tables XI, XII, and XIII. In all cases, the two-group XS error decreased by more than 67%. Particularly, the down-scattering and thermal group XS error decreased by more than 88%. The APEC-SI method showed further improvement in the accuracy of fast group fission XS and down-scattering XS.

Table VIII. Nodal calculation results (variant core 1)

	$k_{eff}$	$\Delta\rho$ (pcm)	assembly power RMS error (%)	assembly power Max. error(%)
DeCART2D	1.148344	-	-	-
FWC	1.149522	89.2	1.36	-2.53
APEC	1.148905	42.5	0.72	-1.15
APEC-SI	1.148603	19.6	0.67	-1.03
Ref. XS	1.148298	-3.5	0.64	-1.14

Table IX. Nodal calculation results (variant core 2)

	$k_{eff}$	$\Delta\rho$ (pcm)	assembly power RMS error (%)	assembly power Max. error(%)
DeCART2D	1.144304	-	-	-
FWC	1.145486	90.2	1.57	-2.67
APEC	1.144152	-11.6	0.61	1.33
APEC-SI	1.144259	-3.5	0.63	1.47
Ref. XS	1.144073	-17.6	0.59	1.30

Table X. Nodal calculation results (variant core 3)

	$k_{eff}$	$\Delta\rho$ (pcm)	assembly power RMS error (%)	assembly power Max. error(%)
DeCART2D	1.146231	-	-	-
FWC	1.147416	90.1	1.05	2.13
APEC	1.146471	18.2	0.94	-1.47
APEC-SI	1.146269	2.9	0.82	-1.33
Ref. XS	1.146147	-6.4	0.80	-1.37

Table XI. RMS error of assembly-wise CFR and XS (variant core 1)

	FWC (%)	APEC (%)	APEC-SI (%)	Ref. XS (%)
CFR <sub>1</sub>	7.05	15.04	15.41	9.65
CFR <sub>2</sub>	18.62	11.09	13.20	10.24
D <sub>1</sub>	0.34	0.11	0.12	0.00
D <sub>2</sub>	0.32	0.03	0.02	0.00
$\Sigma_{a1}$	0.34	0.05	0.04	0.00
$\Sigma_{a2}$	0.53	0.04	0.03	0.00
$v\Sigma_{f1}$	0.54	0.10	0.07	0.00
$v\Sigma_{f2}$	0.77	0.06	0.06	0.00
$\Sigma_{s1\rightarrow 2}$	1.06	0.11	0.06	0.00
$\Sigma_{s2\rightarrow 1}$	2.79	0.23	0.22	0.00

Table XII. RMS error of assembly-wise CFR and XS (variant core 2)

	FWC (%)	APEC (%)	APEC-SI (%)	Ref. XS (%)
CFR <sub>1</sub>	6.93	10.31	9.78	8.77
CFR <sub>2</sub>	38.67	29.16	30.32	31.17
D <sub>1</sub>	0.35	0.11	0.12	0.00
D <sub>2</sub>	0.26	0.03	0.03	0.00
Σ <sub>a1</sub>	0.36	0.03	0.04	0.00
Σ <sub>a2</sub>	0.36	0.04	0.03	0.00
vΣ <sub>f1</sub>	0.47	0.12	0.10	0.00
vΣ <sub>f2</sub>	0.65	0.07	0.07	0.00
Σ <sub>s1→2</sub>	0.92	0.08	0.07	0.00
Σ <sub>s2→1</sub>	2.79	0.23	0.22	0.00

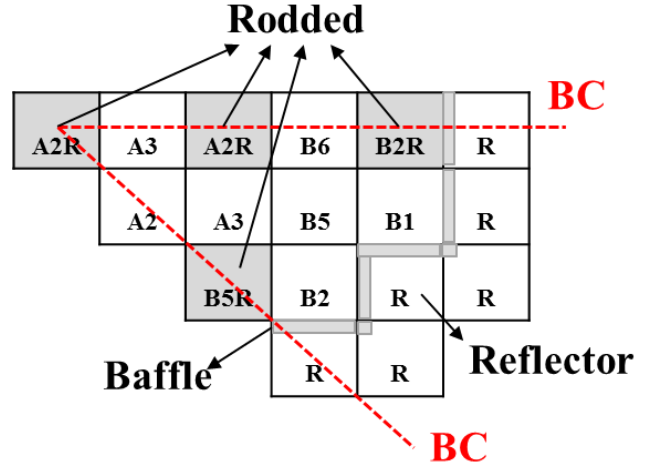


Fig. 13. Core configuration of the rodDED core

Table XIII. RMS error of assembly-wise CFR and XS (variant core 3)

	FWC (%)	APEC (%)	APEC-SI (%)	Ref. XS (%)
CFR <sub>1</sub>	9.87	23.56	22.16	21.71
CFR <sub>2</sub>	15.17	24.00	24.20	24.73
D <sub>1</sub>	0.36	0.10	0.11	0.00
D <sub>2</sub>	0.22	0.04	0.03	0.00
Σ <sub>a1</sub>	0.36	0.04	0.04	0.00
Σ <sub>a2</sub>	0.36	0.03	0.03	0.00
vΣ <sub>f1</sub>	0.48	0.10	0.07	0.00
vΣ <sub>f2</sub>	0.54	0.05	0.05	0.00
Σ <sub>s1→2</sub>	0.95	0.10	0.06	0.00
Σ <sub>s2→1</sub>	2.12	0.25	0.23	0.00

Table XIV. SMR core color-set models for basic APEC method

Type of color-set model	Set of FAs in color-set (FA1, FA2)
Checkerboard	(A2,A3), (A2,B5), (A2,B5R), (A2R,A3), (A2R,B5), (A3,B6), (B5,B1), (B5R,B1), (B5R,B6), (B6,B1)
Flat baffle	(B2R,A2), (B2R,B2), (B2R,B6)
L-shape baffle	(B1,A2), (B1,B1), (B1,B5), (B2,A2), (B2,B2), (B2,B6), (B2,B5R)

### B. RodDED core test

A rodDED SMR initial core is tested to determine the performance of the APEC method in extreme conditions with very strong neighborhood effects. Figure 13 shows the position of rodDED assemblies in the problem. The lattice calculations of the rodDED FA were added to the lattice calculation used in the previous SMR initial core analysis. Nine single assembly calculations are performed including three rodDED FAs (A2R, B2R, B5R). Similar to the single FA calculations, color-set calculations have been performed to consider rodDED FAs. 20 color-set calculations have been performed for the basic APEC function fitting as shown in Table XIV and 12 additional color-set calculations have been performed for the APEC-SI function fitting as shown in Table XV.

Table XV. Additional color-set models for APEC-SI method (FA1, FA2)

Type of color-set model	Set of FAs in color-set (FA1, FA2)
Checkerboard	(A2,A2R), (A2,B1), (A2,B6), (A2R,B1), (A2R,B2), (A2R,B6), (A3,B1), (A3,B5), (A3,B5R), (B5,B5R), (B5,B6), (B5R,B2)

The nodal calculation condition of the control rod inserted SMR initial core is the same as that of the core without control rods inserted except for the FA two-group XS. The APEC methods significantly improved the accuracy of the nodal calculations, as shown in Table XVI. When comparing the results using the conventional FWC and the APEC method, the reactivity error is reduced by more than 77%, the assembly power RMS error reduced by more than 69%, and the assembly power maximum error is also reduced by more than 62%. However, the improved APEC method did not show any further improvement over the basic APEC method.

Table XVI. Nodal calculation results (variant core 3)

	$k_{eff}$	$\Delta\rho$ (pcm)	assembly power RMS error (%)	assembly power Max. error(%)
DeCART2D	1.146231	-	-	-
FWC	1.147416	90.1	1.05	2.13
APEC	1.146471	18.2	0.94	-1.47
APEC-SI	1.146269	2.9	0.82	-1.33
Ref. XS	1.146147	-6.4	0.80	-1.37

Comparing the assembly normalized power distribution, the effect of the APEC XS correction is more noticeable. While the reference assembly normalized power distribution from the DeCART2D calculation is shown in Fig. 14, the assembly power error distribution is shown in Fig. 15. The control rod inserted FAs have particularly low assembly power and the relative error of the power is large when using conventional FWC. However, when the APEC method is applied, the power distribution error of the control rod inserted FA at the inner core region (close to 9.9%) is reduced to less than 1%. The APEC method shows a similar power distribution to that using the reference XS.



Fig. 14. Reference assembly normalized power distribution of the rodded core

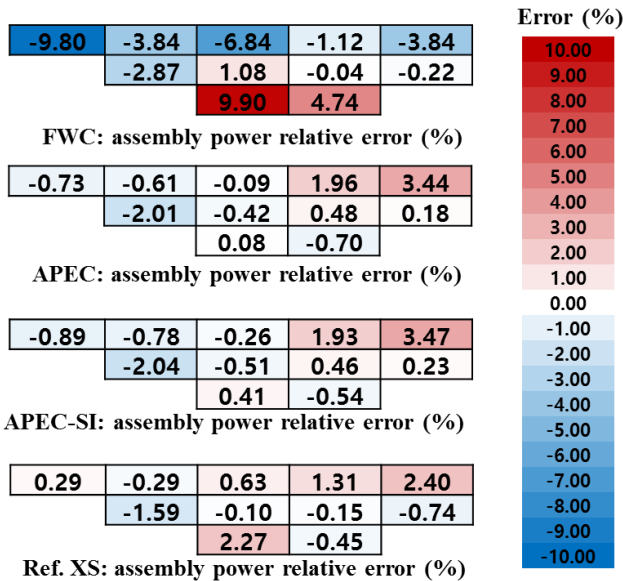


Fig. 15. Relative error of assembly normalized power distribution of the rodded core

In Table XVII, the FA two-group XS relative error is compared. It is shown that the APEC XS correction performs well in all FAs by comparing the RMS error. In the single FA calculation, the control rod inserted FA is surrounded by other FAs with the control rods inserted, a serious deviation from the actual core. This produces a serious XS error that can be largely resolved by using the APEC method. When the control rod is inserted into the FA, the two-group XS of the surrounding FA differ greatly in addition to the control inserted FA. The APEC method can effectively reduce the error in such surrounding FAs. On the other hand, the APEC XS correction did not yield an accurate CFR. However, even the reference the XS could not yield accurate CFRs. This is due to the large ADF error.

Table XVII. RMS error of assembly-wise CFR and XS (variant core 1)

	FWC (%)	APEC (%)	APEC-SI (%)	Ref. XS (%)
<b>CFR<sub>1</sub></b>	7.05	15.04	15.41	9.65
<b>CFR<sub>2</sub></b>	18.62	11.09	13.20	10.24
<b>D<sub>1</sub></b>	0.34	0.11	0.12	0.00
<b>D<sub>2</sub></b>	0.32	0.03	0.02	0.00
<b>Σ<sub>a1</sub></b>	0.34	0.05	0.04	0.00
<b>Σ<sub>a2</sub></b>	0.53	0.04	0.03	0.00
<b>vΣ<sub>f1</sub></b>	0.54	0.10	0.07	0.00
<b>vΣ<sub>f2</sub></b>	0.77	0.06	0.06	0.00
<b>Σ<sub>s1→2</sub></b>	1.06	0.11	0.06	0.00
<b>Σ<sub>s2→1</sub></b>	2.79	0.23	0.22	0.00

#### IV. CONCLUSIONS

A new leakage correction method named APEC has been developed to improve the standard homogenized two-group XSs for PWR fuel assemblies. The two-group XSs can be well formulated as a function of an integrated albedo information current-to-flux ratio (CFR) on the boundary. The fast group XS corrections are found to have a linear dependence on both fast and thermal group CFRs, while thermal XS correction can be well modeled by a quadratic function of the thermal group CFR only. For accurate parameterization of the XS, several color-set problems should be analyzed with a marginal increase in the total computational cost. By using color-set models, realistic assembly interface transport effects are included in the parameterization. If a FA neighbors the baffle and water reflector, it is necessary to consider the baffle-reflector region in the color-set models for the APEC function.

Application of the APEC method to an SMR core showed that the APEC method provided very accurate position dependent two-group XSs and nodal accuracy was improved to match the two-group XS accuracy. In particular,

several tests are performed using various cores in order to see the generality of the APEC method. The performance of the APEC method in any core configuration was as good as in the original core configuration and showed that the use of well-defined APEC functions can be generally applied to various core configurations. Also, nodal analysis for the control rod inserted SMR initial core showed the advantages of the APEC method in abnormal operating conditions.

Although the total calculation time for the lattice calculation is increased by the addition of color-set models, it is still acceptable considering the computational efficiency of the two-step procedure. Once the color-set model included lattice calculations are performed with some additional effort, the resulting Xs and APEC parameters can be used repeatedly for high accuracy core nodal calculations without extra computing cost. Even though numerous nodal calculations will be performed in core design and transient core simulations, the additional computing time due to the use of the color-set model in the lattice calculation is small.

The computing time for the color-set models will be still acceptable even when fuel depletion is considered. In the APEC method lattice calculations, depletion calculations will be performed using the conventional infinite lattice model. After the depletion calculations are over, color-set models are chosen including FAs with various burnup. The process is similar to branch calculations for T/H feedback with a marginal increase in computing time. The APEC method including fuel depletion has not been tested yet and will be discussed in future works. In addition, the functionalization of the discontinuity factor is left to future development of the APEC method.

## ACKNOWLEDGMENTS

This work was supported by the National Research Foundation of Korea (NRF) Grant funded by the Korean Government (MSIP) (NRF-2016R1A5A1013919).

## REFERENCES

1. K. S. SMITH, "Assembly Homogenization Techniques for Light Water Reactor Analysis, Progress in Nuclear Energy," 17(3), 303-335, (1986).
2. R. J. STAMMLER, "HELIOS Methods," Studsvik Scanpower, (1998).
3. K. T. CLARNO and M. L. ADAMS, "Capturing the Effect of Unlike Neighbors in Single-Assembly Calculations," Nuclear science and engineering, 149(2), 182-196, (2005).
4. W. HEO and Y. KIM, "Position-dependency of Fuel Assembly Homogenization in a Pressurized Water Reactor," Transactions of ANS 2016, Vol. 114, New Orleans, USA, June 12-16, (2016).
5. F. RAHNEMA, NICHITA E.M., "Leakage corrected spatial (assembly) homogenization technique," Annals of Nuclear Energy 24 (6), 477-488, (1997).
6. F. RAHNEMA, M. S. MCKINLEY, "High-order cross-section homogenization method," Annals of Nuclear Energy, 29(7), 875-899, (2002).
7. J. J. HERRERO et al., "Neighborhood-corrected interface discontinuity factors for multi-group pin-by-pin diffusion calculations for LWR," Annals of Nuclear Energy, 46, 106-115, (2012).
8. S. P. PALMTAG, "Advanced Nodal Method for MOX Fuel Analysis", Ph.D. Thesis, Massachusetts Institute of Technology, (1997).
9. Y. S. BAN and J. G. JOO, "LEAKAGE CORRECTION OF HOMOGENIZED FEW-GCS THROUGH FUNCTIONALIZATION ON LEAKAGE FRACTION", PHYSOR 2016, Sun Valley, ID, May 1-5, (2016).
10. W. KIM and Y. KIM, "Feasibility of Nodal Equivalence Theory Using Functionalized Homogenized Parameters," Trans. Am. Nucl. Soc., Vol. 110, Reno, NV, US, June 15-19, (2014).
11. W. KIM and Y. KIM, "Feasibility of Albedo-corrected Parameterized Equivalence Constants for Nodal Equivalence Theory," ANS M&C+SNA+MC 2015, Nashville, TN, April 19-23, (2015).
12. W. KIM and Y. KIM, "Albedo-corrected Parameterized Equivalence Constants for Cross-section Update in Nodal Calculation", Proceedings of the Korean Nuclear Society Autumn Meeting, Gyeongju, Oct 27-28, (2016)
13. J. Y. CHO, "DeCART2D v1.1 User's Manual," KAERI/UM-40/2016, (2016)
14. S. SONG, "Pin-by-Pin Core Calculation with NEM-Based Two-Level CMFD Algorithm", Master's Thesis, KAIST, (2016).
15. J. J. DUDERSTADT and L. J. HAMILTON, "Nuclear Reactor Analysis," John Wiley & Sons, Inc., New York, (1976).
16. K. S. SMITH and J. D. RHODES III, "CASMO Characteristics Method for Two-Dimensional PWR and BWR Core Calculation," Trans. Am. Nucl. Soc., 83, 294, (2000).
17. N. Z. CHO, "On a New Acceleration Method for 3D Whole-Core Transport Calculations," Annual Mtg. Atomic Energy Society of Japan, Sasebo, Japan, March 27-29, 2003, Atomic Energy Society of Japan, (2003).
18. N. Z. CHO, "The Partial Current-Based CMFD (p-CMFD) Method Revisited," Transactions of the Korean Nuclear Society Autumn Meeting, Gyeongju, Korea, October 25-26, (2012).
19. S. YUK and N. Z. CHO, "Shifting and Two-Level Iterative Techniques to Speedup p-CMFD Acceleration in Transport Calculation," Transactions of the Korean Nuclear Society Autumn Meeting, Gyeongju, Korea, October 27-28, (2016).